



## Selective detection of alpha synuclein amyloid fibrils by faradaic and non-faradaic electrochemical impedance spectroscopic approaches

Hussaini Adam<sup>a</sup>, Subash C.B. Gopinath<sup>a,b,c,d,e,f,\*</sup>, Hemavathi Krishnan<sup>a</sup>, Tijjani Adam<sup>a,g</sup>, Makram A. Fakhri<sup>h</sup>, Evan T. Salim<sup>i</sup>, A. Shamsher<sup>j</sup>, Sreeramanan Subramaniam<sup>a,c,e,k</sup>, Yeng Chen<sup>l</sup>

<sup>a</sup> Institute of Nano Electronic Engineering, Universiti Malaysia Perlis (UniMAP), 01000 Kangar, Perlis, Malaysia

<sup>b</sup> Center for Global Health Research, Saveetha Medical College & Hospital, Saveetha Institute of Medical and Technical Sciences (SIMATS), Thandalam, Chennai 602 105, Tamil Nadu, India

<sup>c</sup> Faculty of Chemical Engineering & Technology, Universiti Malaysia Perlis (UniMAP), 02600 Arau, Perlis, Malaysia

<sup>d</sup> Department of Technical Sciences, Western Caspian University, Baku, AZ 1075, Azerbaijan

<sup>e</sup> Centre for Chemical Biology, Universiti Sains Malaysia, Bayan Lepas, 11900 Penang, Malaysia

<sup>f</sup> Department of Computer Science and Engineering, Faculty of Science and Information Technology, Daffodil International University, Daffodil Smart City, Birulia, Savar, Dhaka 1216, Bangladesh

<sup>g</sup> Faculty of Electronic Engineering & Technology, Universiti Malaysia Perlis, 02600 Arau, Perlis, Malaysia

<sup>h</sup> Laser and Optoelectronics Eng. Department, University of Technology-Iraq, Baghdad 10066, Iraq

<sup>i</sup> Applied Science Department, University of Technology-Iraq, Baghdad 10066, Iraq

<sup>j</sup> Electrical Engineering Department, Seberang Perai Polytechnic, 13500 Permatang Pau, Penang, Malaysia

<sup>k</sup> School of Biological Sciences, Universiti Sains Malaysia, Georgetown, 11800 Penang, Malaysia

<sup>l</sup> Department of Oral and Craniofacial Sciences, Faculty of Dentistry, Universiti Malaya, Kuala Lumpur 50603, Malaysia

### ARTICLE INFO

#### Keywords:

Amyloid alpha  
Amyloid fibrils  
Electrochemical impedance  
Biosensor  
Parkinson's disease

### ABSTRACT

This study utilized faradaic and non-faradaic electrochemical impedance spectroscopy to detect alpha synuclein amyloid fibrils on gold interdigitated tetraelectrodes (AuIDTE), providing valuable insights into electrochemical reactions for clinical use. AuIDTE was purchased, modified with zinc oxide for increased hydrophobicity. Functionalization was conducted with hexacyanidoferrate and carbonyldiimidazole. Faradaic electrochemical impedance spectroscopy has been extensively explored in clinical diagnostics and biomedical research, providing information on the performance and stability of electrochemical biosensors. This understanding can help develop more sensitive, selective, and reliable biosensing platforms for the detection of clinically relevant analytes like biomarkers, proteins, and nucleic acids. Non-faradaic electrochemical impedance spectroscopy measures the interfacial capacitance at the electrode–electrolyte interface, eliminating the need for redox-active species and simplifying experimental setups. It has practical implications in clinical settings, like real-time detection and monitoring of biomolecules and biomarkers by tracking changes in interfacial capacitance. The limit of detection (LOD) for normal alpha synuclein in faradaic mode is 2.39-fM, The LOD for aggregated alpha synuclein detection is 1.82-fM. The LOD for non-faradaic detection of normal alpha synuclein is 2.22-fM, and the LOD for non-faradaic detection of aggregated alpha synuclein is 2.40-fM. The proposed EIS-based AuIDTEs sensor detects alpha synuclein amyloid fibrils and it is highly sensitive.

### 1. Introduction

Alpha synuclein amyloid fibrils are protein aggregates linked to neurodegenerative disorders like Parkinson's disease [1]. Detecting and quantifying these fibrils is crucial for understanding disease progression

and developing targeted therapies. Accurate quantification can identify potential drug targets and aid early detection. Electrochemical impedance spectroscopy is a promising method for selectively detecting fibrils [2]. Electrochemical impedance spectroscopy is a promising method for identifying and characterizing fibrils by understanding their electrical

\* Corresponding author at: Institute of Nano Electronic Engineering, Universiti Malaysia Perlis, 01000 Kangar, Perlis, Malaysia.

E-mail address: [subash@unimap.edu.my](mailto:subash@unimap.edu.my) (S.C.B. Gopinath).

<https://doi.org/10.1016/j.bioelechem.2024.108800>

Received 28 January 2024; Received in revised form 19 August 2024; Accepted 21 August 2024

Available online 30 August 2024

1567-5394/© 2024 Elsevier B.V. All rights are reserved, including those for text and data mining, AI training, and similar technologies.

properties and interactions with electrode surfaces. Alpha synuclein is a protein that is crucial in neurodegenerative disorders like Parkinson's disease and dementia with Lewy bodies [3]. Parkinson's disease is a neurodegenerative disorder affecting the geriatric population, characterized by selective vulnerability of neurons, leading to deterioration and impaired functioning of specific neuronal cells [4]. Alpha synuclein amyloid fibrils are crucial in the disease's aetiology, impairing cellular functions and causing the condition's onset [5]. The progressive destruction of dopaminergic neurons can cause movement deficits, affecting everyday activities [6]. These impairments include quivering or tremor at rest, sluggishness, rigid musculature, and instability in maintaining proper posture. Detection of alpha-synuclein is essential for early diagnosis and monitoring of these diseases [7]. Alpha synuclein amyloid fibrils have been suggested as potential biomarkers for neurodegenerative diseases like Alzheimer's, Parkinson's, and Lewy body dementia [8]. The detection and characterization of Alpha synuclein amyloid fibrils in Parkinson's disease are crucial for understanding its pathology and developing diagnostics [9]. These alpha synuclein amyloid fibrils can be found in cerebrospinal fluid and plasma, and their presence and spread are linked to disrupting key cellular processes, including protein production [10]. Research on Parkinson's disease focuses on the detection of alpha synuclein amyloid fibrils which are believed to contribute to the disease's pathogenesis and other neurodegenerative disorders [11]. These alpha synuclein amyloid fibrils disrupt cellular processes like protein trafficking, autophagy, lysosomal function, protein clearance, and synaptic integrity [12]. The spread of these alpha synuclein amyloid fibrils is linked to disease progression [13]. Various methods have been developed to detect alpha synuclein amyloid fibrils, however these often require complex instruments and are time-consuming [14]. Hence, electrochemical impedance spectroscopy has emerged as a promising technique [15]. This technique offers advantages such as simplicity, sensitivity, and real-time based on faradaic and non-faradaic techniques to detect alpha synuclein amyloid fibrils in Parkinson's disease [16]. Biosensors based on electrochemical impedance spectroscopy are widely used in culinary, medical, and environmental research. EIS systems use low amplitude alternating current voltages at varied frequencies to measure the response of chemical processes [17]. A working, reference, and counter electrode combination transfers a known voltage from the working electrode to the counter electrode through an electrolytic solution [18]. An electrochemical spectrometer is electrically connected to an electrochemical cell containing the chemical process to acquire the electrical response of an electrolytic solution [18]. EIS systems are operated by computer software designed specifically for EIS testing, therefore, the software components must be installed before starting an experiment [19]. The electrolytic solution is poured into a sample container, and if a metallic container provides extra electron pathways, the EIS current response decreases during testing [20]. Further, non-faradaic EIS and faradaic EIS are two types of EIS-based biosensors that are affected by the presence or absence of redox reagents [21]. The non-faradaic-EIS sensor is based on capacitance changes at the electrode-electrolyte interface and uses a redox-free electrolyte, while the faradaic-EIS-based sensor uses a charge transfer process between the electrodes and the redox reagent. The article introduces an Electronic Insight System (EIS) method to enhance the sensitivity of an interdigitated tetraelectrodes (AuIDTEs) sensor for the detection of amyloid alpha synuclein. The sensing technique lowers alpha synuclein aggregation by adjusting the buffer solution. Electrochemical impedance spectroscopy (EIS) is a biosensor method that examines the electrical characteristics of the electrode surface electrochemically. Biosensors on electrode surfaces detect changes in biosensors and the kinetics of molecules like DNA, receptors, antibodies, antigens, and proteins [22]. EIS-based biosensor systems could potentially assist in the detection of Parkinson's disease biomarkers [23]. Table 1 presents a comparison of various bioreceptors found on biosensor surfaces. In this study, MEMS technology was used to create the Interdigitated tetraelectrodes (AuIDTEs) sensor, which was

**Table 1**  
Comparison of several bioreceptors in biosensor surfaces.

Bioreceptor	Advantage	Disadvantage	Reference
DNA/ Aptamer	Excellent selectivity, specificity, and a broad application range	Substantial cost and labelling are required.	[25]
Antibody	Excellent sensitivity, specificity, and a wide range of applications	Polyclonal and monoclonal antibodies have low thermal stability, a high price, and are immunogenic.	[26]
Enzyme	Low cost, structure introduced, sensitivity, and simplicity	Poor thermal and pH stability chemical and often interferences	[27]
Whole cell	Long life-span low cost, a diverse range of enzymes, and thermal stability	Slow response and limited selectivity	[28]

evaluated by observing impedance fluctuations produced by different concentrations of alpha synuclein under faradaic and non-faradaic settings. Table 2 compares the advantages, disadvantages, detection ranges, and limits of faradaic and non-faradaic Electrochemical Insights (EIS) techniques. Faradaic EIS is ideal for studying redox reactions, charge-transfer kinetics, and corrosion processes, however, requires a redox-active species in the electrolyte, making it limited to certain systems [18]. Non-faradaic EIS is more versatile and can investigate a wider range of systems, including those without redox-active species [24]. It typically covers a broader frequency range, allowing for analysis of both slow and fast electrochemical processes. The choice between these techniques depends on the specific requirements of the system and the information sought.

## 2. Experimental

### 2.1. Materials and reagents

Interdigitated tetraelectrodes (AuIDTEs) was purchased from Metrohm, Malaysia, developed at 10  $\mu\text{m}$  gap. Metrohm (Malaysia). From Sigma Aldrich (USA), alpha-synuclein (diluted to attomolar–picomolar concentrations),  $[\text{C}_7\text{H}_6\text{N}_4\text{O}$ , 162.15 g/mol, powder or crystals or chunk (s), solubility: clear to very slightly hazy. Ethanolamine  $[\geq 99.0\% \text{C}_2\text{H}_7\text{NO}$ , 61.08 g/mol, colorless, liquid or viscous liquid] and human serum were purchased. The antibody was also purchased from Promega, United States. The concentration of antibody for the probe immobilization was 100 nM. Ethanolamine at 1 M concentration was used as a blocking agent. 0.5 mM Carbonyldiimidazole (CDI) was prepared and dropped on the surface of the gold interdigitated tetraelectrodes (AuIDTEs). The purpose of using CDI was to activate the surface of the gold interdigitated tetraelectrodes (AuIDTEs) so that antibodies could be attached. This allows for the creation of strong covalent bonds between the antibody and the sensor surface, resulting in a stable and effective biosensor. Phosphate buffered saline (PBS) at pH 7.4 was from Sigma Aldrich, USA, used at 10 mM concentration.

### 2.2. Pretreatment and characterization on AuIDTEs based biosensor

The device was pretreated by washing it with DI water and allowing it to dry. The device was then submerged in a diluted concentrated  $\text{H}_2\text{SO}_4$  solution for 10 min before being dried. A high-power microscope model Olympus BX5, 3D-nanoprofler, scanning electron microscopy were used for the sensor characterizations. The size and dimensions of the biosensor and its electrode elements were defined using a scanning electron microscope, high power microscope, and a 3D Profilometer was utilized to measure areal surface topography. The working electrode

**Table 2**

Advantages and disadvantages, detection ranges, and limits of faradaic and non-faradaic EIS techniques.

Electrode structure	Technique	Linear range	Detection limit	Advantage	Disadvantage	Reference
Surface imprinted polymer (SIP)	Faradaic and non-faradaic EIS	5 pg/L–5 µg/L	5 pg/L	The low-cost and are highly suitable for non-invasive monitoring of disease biomarkers	The binding between SIP and target biomolecule only relies on steric forces, which are significantly influenced by high energy media components in complex media like whole blood, serum, or interstitial fluid biological samples	[29]
Field-Effect Transistor integrated with microfluidics	Faradaic and non-faradaic EIS	0.25 pM–25 nM	0.25 pM	Offer a label-free tool for studying protein aggregation	The sensor was not suitable for a large number of samples	[30]
Reduced graphene oxide	Faradaic EIS	1 fM–1 nM	0.64 fM	High sensitivity and selectivity	The proposed biosensor is not suitable for multi-shot sensing due to its slow response.	[31]
Carbon nanotube	Faradaic EIS	1–25 ng/mL	200 pg/mL	High sensitivity	Derived assays face challenges in reliably generating specific signals in complex media	[32]
Carbon screen-printed electrodes	Faradaic EIS	1 fM–10 pM	1 fM	The sensor showed great analytical performance in alpha-synuclein detection	Screen-printing process may result in a decrease in the active electrode area, which can affect the adsorption properties and reproducibility of the electrode.	[33]
Interdigitated microelectrode	Faradaic EIS	0.1–100 pg/mL	7.4-fold	The proposed method effectively utilizes faradaic spectroscopy with high-sensitivity	The f-EIS sensor's redox reagent incorporation makes it challenging to detect specific biomolecules like amyloid beta.	[34]
Carbon black to a poly	Non-faradaic EIS	6.0–100.5 µg mL <sup>-1</sup>	1.3 µg mL <sup>-1</sup>	The sensor exhibited low limit of detection	The sensor is not suitable for long-term applications	[35]
molecularly imprinted polypyrrole	Faradaic EIS	1 nM–500 nM)	1 nM	The sensors demonstrated broad detection range, good stability, and higher sensitivity	The limit of detection is high	[36]
Molecularly imprinting polymer platinum electrodes	Faradaic EIS	1 µM–500 µM	0.4 µM	Low cost and high sensitivity	The sensor is not suitable for a real human sample.	[37]
	Faradaic EIS	3.5 × 10 <sup>-5</sup> mol/L–8.0 × 10 <sup>-4</sup> mol/L	5.1 × 10 <sup>-6</sup> mol/L	The proposed sensor is suitable as an alternative method for diagnosing this disease	The sensor lacks selectivity and reproducibility	[38]
PPy@NU-1000	Faradaic EIS	0.005–70 µM	0.0001 µM	The sensor described is highly sensitive, stable, and reproducible	The sensor's performance decreases in the presence of do-pamine (>0.5 mM) and requires a 10-time dilution for practical sample analyzation	[39]

area was 1.54 mm<sup>2</sup>, and it was able to accommodate 20–25 µL of liquid test sample. The biosensing response was characterised using electrochemical surface area stability and repeatability. EIS measurements were conducted in 0.1 M Fe(CN)<sub>6</sub>]<sub>3</sub> solutions. Impedance analyzer was used to conduct the electrochemical impedance spectroscopy measurements.

### 2.3. Pretreatment of alpha synuclein monomer

Pretreatment was conducted by dissolving in glycine–NaOH buffer at

a pH of 7.4, then incubating for five days at 37 °C with minimal agitation. The resulting fibril was kept at 4 °C until storage. Aggregated protein preparation was prepared in concentrations ranging from 1 pM to 1 aM using the agitated buffer solution.

### 2.4. Measurements

The study investigated the sensing mechanism of alpha synuclein amyloid fibrils through EIS tests using antibody-modified Interdigitated tetraelectrodes (AuIDTEs) in the presence of increasing amounts of

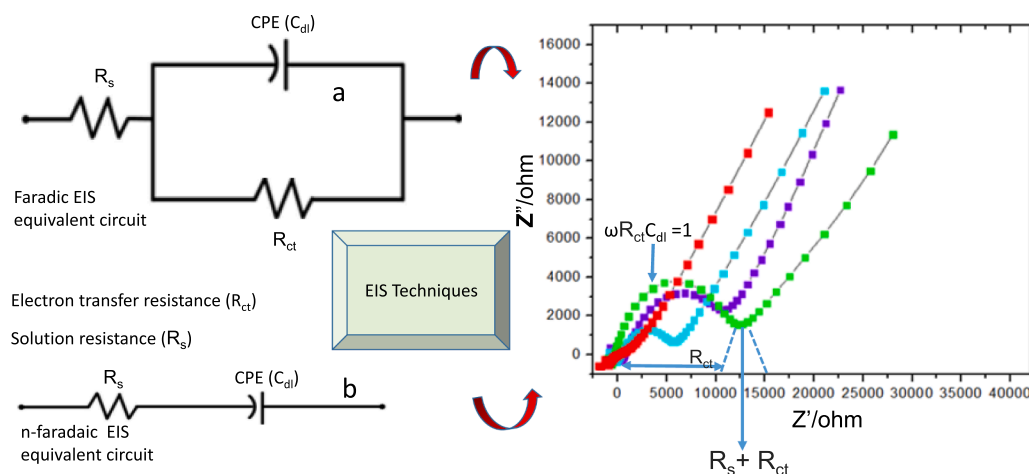


**Fig. 1.** Faradaic and non-faradaic techniques: (a) Depicts the matching circuit of the faradaic-EIS-based interdigitated tetraelectrodes (AuIDTEs) sensor. (b) Depicts the matching circuit of the non-faradaic-EIS-based interdigitated tetraelectrodes (AuIDTEs) sensor.

alpha synuclein concentrations. A gold electrode with a diameter of 2 mm was incubated in a PBS solution containing 10 M antibody. After cleaning the electrode with ethanol/water, a concentration of alpha synuclein was cast onto the sensor surface for 30 min. The electrode was submerged in a solution of  $[\text{Fe}(\text{CN})_6]_3$  (1:1) for impedance measurement. Fig. 1a depicts the matching circuit of the faradaic-EIS-based interdigitated tetraelectrodes AuIDTEs sensor. The presence or absence of redox reaction was used to classify non-faradaic and faradaic EIS-based biosensors. Randles equivalent circuit models of the two approaches were compared with experimentally recorded impedance spectra.  $R_{ct}$  denotes the charge transfer resistance caused by the charge transfer process between the redox reagent and the electrodes. A novel detection approach was reported employing two types of buffers: one containing the redox reagent (faradaic) for measuring impedance before and after the immunoassay, and one containing alpha synuclein in PBS buffer (non-faradaic) for the alpha synuclein immunoassay. The non-faradaic-EIS contains a solution resistance  $R_s$  as well as a constant phase element (CPE) (Fig. 1b).

## 2.5. Overall research design

This study detects alpha synuclein amyloid fibrils by comparing faradaic and non-faradaic EIS techniques (Fig. 2). Furthermore, this shows how the antibody is immobilized onto the electrode surface. This step is important because it determines the performance and stability of the biosensor. Buffers were only used for preparing the sensing area, where both the antibody and target protein are present. The highest concentration of the target was compared control protein (Tau) for selectivity analysis. A scanning electron microscopy, a higher power microscope, a 3D profilometer, and an atomic force microscope were used to characterise the samples. For target analysis and detection, the antibody was immobilised on AuIDTEs and inhibited using Ethanolamine. The target was then detected by immobilising alpha synuclein for normal and fibrils produced alpha synuclein on antibody modified-AuIDTEs and measuring after washing with  $\text{Fe}(\text{CN})_6]_3$ . The detection of alpha synuclein amyloid fibrils using faradaic and non-faradaic approaches were conducted, which resulted in limit of detection, sensitivity, selectivity, and repeatability.

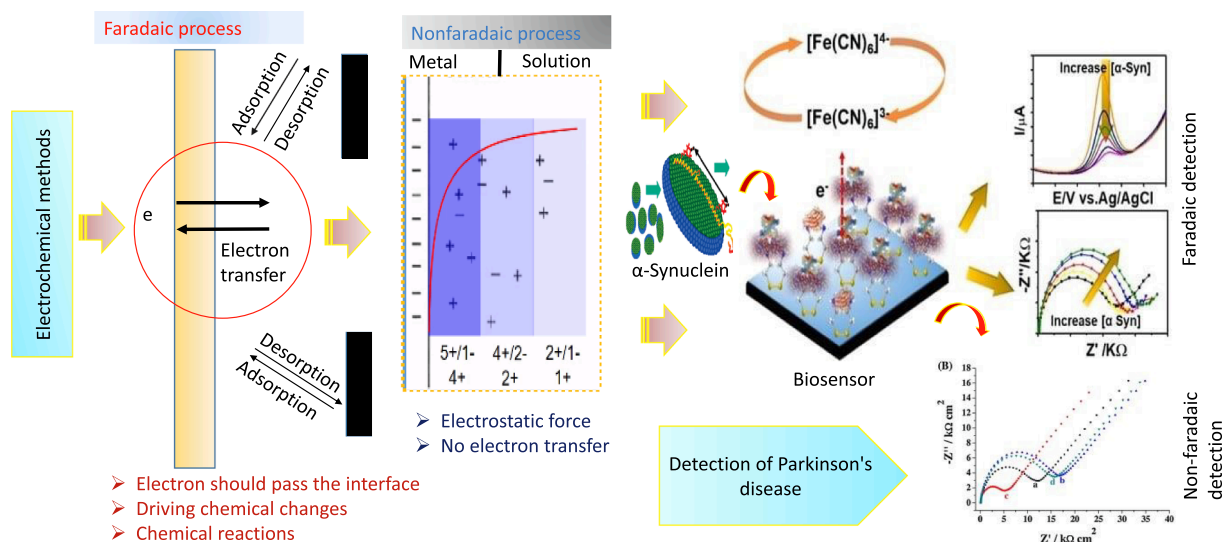


**Fig. 2.** Overall schematic diagram. Physical and electrical characterizations were performed using a scanning electron microscope, a higher power microscope, a 3D profilometer, and current–voltage measurements. AuIDTEs surface functionalization was used to identify normal and amyloid fibrils, alpha synuclein, and AuIDTEs. Antibody was immobilised on the AuIDTEs for target analysis and detection, and the loosely attached surfaces were occluded using Ethanolamine. The target was then detected by immobilising alpha synuclein for normal and oligomer produced alpha synuclein on antibody modified-Au IDTEs and measuring after washing with  $\text{Fe}(\text{CN})_6]_3$ . Faradaic and non-faradaic sensing techniques were employed.

## 3. Results and discussion

### 3.1. Gold interdigitated tetraelectrodes (AuIDTEs)

Gold interdigitated tetraelectrodes (IDTEs) are versatile electrochemical devices used in sensing, electroanalysis, and energy conversion. They consist of four gold-plated interdigitated electrodes arranged in a specific pattern to create a high-density electric field. Their unique design allows for efficient electron capture and transfer, making them ideal for rapid and sensitive electrochemical detection. AuIDTEs also generate high electric fields in a small footprint, making them a key advantage. Hence, a prototype for detecting alpha synuclein aggregation was built on a four-electrode platform biosensor (gold electrode) on a glass substrate with  $10\ \mu\text{m}$  lines and (Fig. 3a). The biosensor's surface topography, dimensions, and electrode components were characterized using a scanning electron microscope. A higher power microscope was used to define the finger electrodes of AuIDTEs electrodes, while areal surface topography and gap surface were determined (Fig. 3b). Areal surface roughness assessment with a 3D Profilometer provides a full view of a surface (Fig. 3c). A high power microscope was utilized to examine the small areas of the electrodes (Fig. 3d). AuIDTE electrodes have a working electrode area of  $1.54\ \text{mm}^2$ . A scanning electron microscope was used to obtain images of the modified AuIDTE electrodes. High-powered microscopy demonstrated that the sensor was perfect.

### 3.2. Impedimetric detection of normal and aggregation of alpha synuclein in Faradaic-EIS and non-Faradaic-EIS techniques

Impedimetric detection is a technique that uses impedance measurements to analyze the presence or concentration of a target molecule or biomarker in a sample. It is highly sensitivity, simple, and label-free. One specific target studied is alpha synuclein, a protein linked to neurodegenerative diseases like Parkinson's. Faradaic impedance spectroscopy measures charge transfer resistance or capacitance changes when the target molecule binds to a specially prepared electrode surface. Non-faradaic impedance spectroscopy measures changes in impedance without redox reactions at the electrode surface. The faradaic-EIS detection approach utilizes Randle's equivalent electronic circuit to analyze and interpret Nyquist data, which displays the imaginary component of impedance against the real component. Nyquist plots

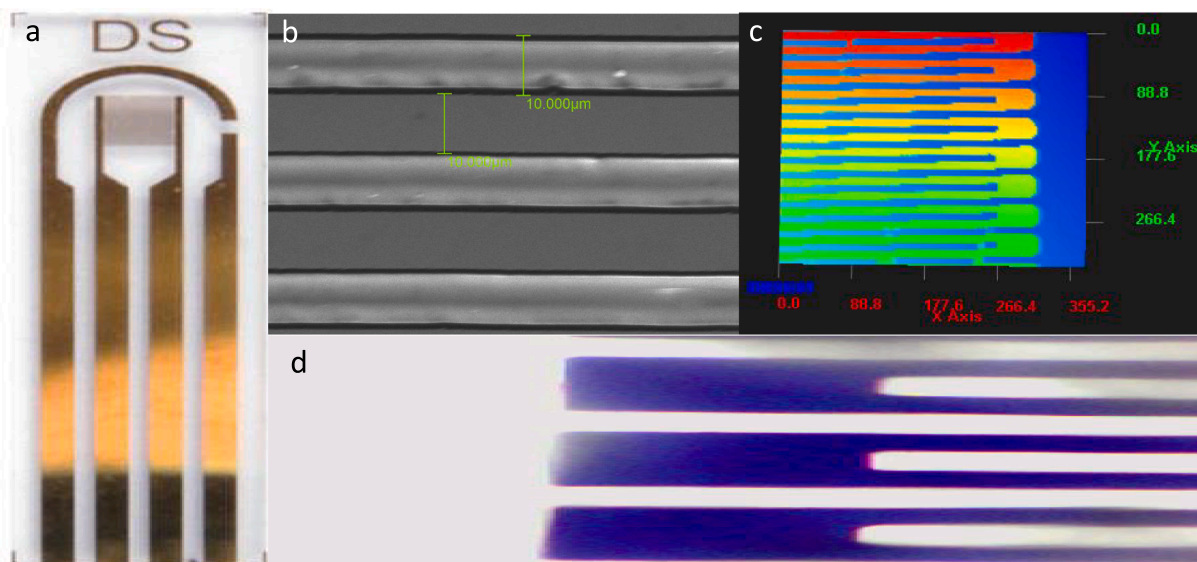


**Fig. 3.** Characterization of gold interdigitated electrodes using higher resolution microscopes: Morphological characterizations of gold interdigitated electrodes were performed using a high-power microscope, scanning electron microscope and 3D Profilometer. (a) Full image of the AuIDTEs, (b) Image of AuIDTEs captured using SEM, (c) Image of AuIDTEs captured using 3D Profilometer, (d) Image of AuIDTEs captured using high power microscope.

provide valuable information about the frequency response of the system and the dynamic process of the electrode. These plots typically show a high-frequency semicircle representing electrolyte solution resistance and a low-frequency slope corresponding to Warburg impedance. Inductive loops in the extremely low frequency region indicate negative values of imaginary impedance. The faradaic-EIS detection approach demonstrates the relationship between real and imaginary impedance components and how changes in the sensing surface affect Rct. As the sensing surface changes, Rct or Z values increase, indicating an increase in sensor surface resistance. This information is crucial for understanding and monitoring the performance of electrochemical systems. The study used AuIDTE to detect and measure the affinity-based interaction between alpha synuclein and antibody using Faradaic-EIS. This technique provides sensitive and quantitative measurements of electrochemical interactions on the AuIDTE electrode surface. This study explores the use of Faradaic-EIS and non-Faradaic-EIS techniques for the

impedimetric detection of normal and aggregated forms of alpha-synuclein, a protein aggregate found in neurodegenerative diseases, and its potential in characterization and detection of biomolecules, including proteins. The study also discusses the charge transfer resistance (Rct) values obtained for the device, which are crucial for understanding charge transfer efficiency at the biosensory interface. For the faradaic detection of normal alpha synuclein, result showed the lowest Rct value of 2.8 kΩ, indicating efficient detection of normal targets (Fig. 4a). However, as the target concentration increased, the Rct values gradually increased. This increase in Rct values suggests that the immobilization procedures and the interaction of the target had an inhibitory effect on the faradaic process of redox and negatively impacted the charge transfer resistance between the solution and the electrode surface. Furthermore, the study demonstrates the use of electrochemical impedance spectroscopy (EIS) in detecting alpha synuclein aggregation in faradaic mode (Fig. 4b). Initially, the device had a

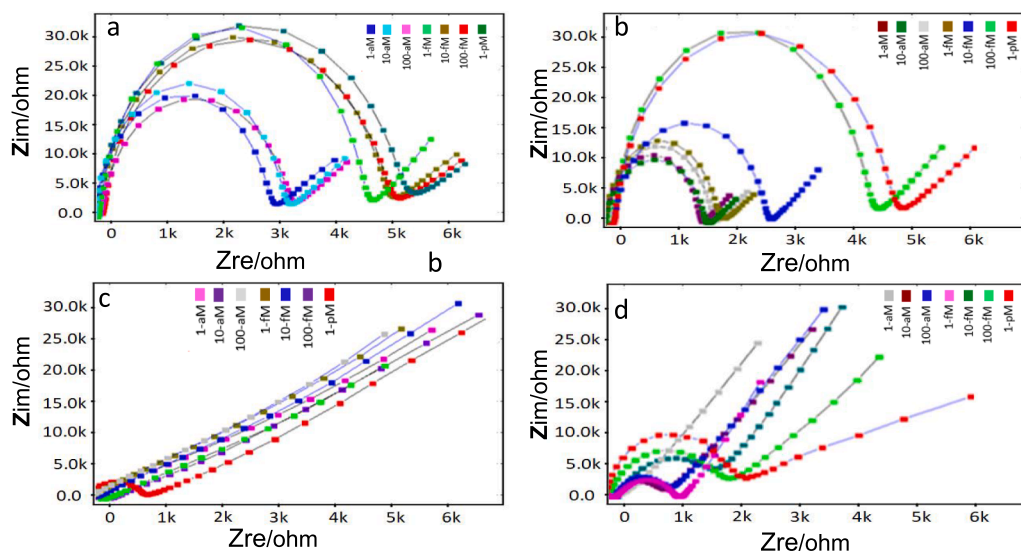


**Fig. 4.** Nyquist response plot of alpha synuclein binding event on biosensing surface, Randleseivalent circuit analysis, electrochemical impedance spectroscopy, Nyquist plot, faradaic, and non-faradaic techniques. (a) faradaic binding of normal alpha synuclein, (b) faradaic binding of aggregated alpha synuclein, (c) non-faradaic binding of normal alpha synuclein (d) non-faradaic binding of aggregated alpha synuclein.

low  $R_{ct}$  value of 1.8 k $\Omega$ , indicating successful detection. However, as the concentration of alpha synuclein increases, the  $R_{ct}$  values increase, indicating an effect on the faradaic process and increased charge transfer resistance. This increase can be attributed to successful immobilization procedures and the target's interaction with electrode surfaces. The study uses Faradaic EIS to detect affinity-based interactions between antibodies and target analytes, revealing the relationship between impedance components and sensor surface resistance. It also analyzes the interaction between alpha-synuclein and AuIDTE to understand its role in alpha synuclein amyloid aggregation. The study also uses  $R_{ct}$  values for non-faradaic detection of alpha synuclein, providing valuable insights into the interaction between the device and target alpha synuclein during non-faradaic detection. The study demonstrates the effectiveness of a device in measuring  $R_{ct}$  values for non-faradaic detection of normal alpha synuclein and its aggregation, as shown in Fig. 4c. The device's ability to measure  $R_{ct}$  values is particularly useful for non-faradaic detection of alpha synuclein amyloid aggregation (Fig. 4d).

### 3.3. Faradaic and non-faradaic biosensing of frequency and magnitude of impedance for normal and aggregated alpha synuclein using AuIDTE

This section discusses faradaic and non-faradaic biosensing of frequency versus total impedance for normal and aggregated alpha synuclein. The plot reveals the relationship between impedance magnitude ( $|Z|$ ) and frequency ( $f$ ), providing insight into the electrochemical processes involved. The analysis of the plot can reveal information about amyloid fibril formation and detection, including the kinetics of amyloid elongation and external factors influencing aggregation. The sensor's Z response curve indicates sensitivity changes in alpha synuclein concentration at frequencies less than  $10^4$  Hz, with surface resistance increasing due to surface and binding processes. Impedance, denoted by the symbol Z, is a measure of resistance to electrical flow. It's measured in ohms. At frequencies over  $10^4$  Hz, the Z response remains constant, where Z is a total impedance, indicating electrolyte resistance, particularly buffer solution. The alpha synuclein binding assay's  $R_{ct}$  value increased to 2.531, indicating effective target interaction. The sensor's activation frequency is around  $10^6$  Hz, with surface resistance increasing through surface pretreatment and binding events. The Z response changed significantly at 9 kHz, 10 kHz, 10.2 kHz, 9.1 kHz, and 5.2 kHz (Fig. 5a). The highest variations were observed at 5.2 kHz, highlighting the need for a development of linear calibration curve. Furthermore, the Z response curves showed continuous resistance at 106 Hz, due to the

buffer solution's electrolyte resistance. Furthermore, Fig. 5b shows the most significant changes in the Z response at 8.1 k, 9 k, 9.1 k, 9.31 k, and 10 kHz frequencies. The Z response curves revealed a constant resistance at 106 Hz. Also, the Z response varied significantly at 10.1 kHz, 10.3 kHz, 10.4 kHz, 10.6 kHz, and 100 kHz (Fig. 5c). The Z response curves showed constant resistance at  $10^6$  Hz. Furthermore, the system's Z response varied significantly at 9.9 kHz, 10.2 kHz, 10.6 kHz, 10.7 kHz, and 102 kHz, allowing the extraction of Z values for the linear calibration curve (Fig. 5d). Hence, this method also allows for label-free detection, eliminating the need for additional chemical labels or tags. The results show a significant increase in total impedance at higher frequencies, indicating the presence of aggregated alpha synuclein. This information can be used to develop diagnostic techniques for diseases associated with abnormal alpha synuclein aggregation, such as Parkinson's disease. AuIDTE can detect subtle changes in affinity-based interactions between primary antibodies and the target analyte, allowing for the detection of alpha synuclein at concentrations below the threshold of other techniques like Raman spectroscopy. This non-faradaic method could be used as a diagnostic tool for alpha synuclein-related diseases, providing valuable insights into aggregation state and potential disease development.

### 3.4. Capacitive detection of alpha synuclein in non-Faradaic EIS and faradaic modes

This study explores the detection of alpha synuclein, both in its normal and aggregated forms, using electrochemical impedance spectroscopy. The study compares the capacitive detection of alpha synuclein in non-Faradaic EIS and faradaic modes. This method utilizes non-faradaic electrochemical impedance spectroscopy to measure the capacitance response of alpha synuclein, allowing for the characterization of alpha synuclein interfaces and their interactions with antibodies. Alpha synuclein interfaces were generated and their antibody recruitment from buffered aqueous solution was characterized before target interaction, leading to more accurate detection of the protein. Fig. 6a–d show the capacitance versus frequency response. Fig. 6a depicts the maximum capacitance of  $30 \times 10^{-6}$  at 1 Hz. Also, Fig. 6b depicts the maximum capacitance of  $29 \times 10^{-6}$  at 5 Hz. Furthermore, at a frequency of 10 Hz, Fig. 6c displays the maximum capacitance of  $28 \times 10^{-6}$ . Finally, Fig. 6d depicts the greatest capacitance of  $31 \times 10^{-6}$  at 10 Hz. As a consequence, the maximum fluctuation in capacitance effect was discovered to be within the frequency range specified. The capacitance

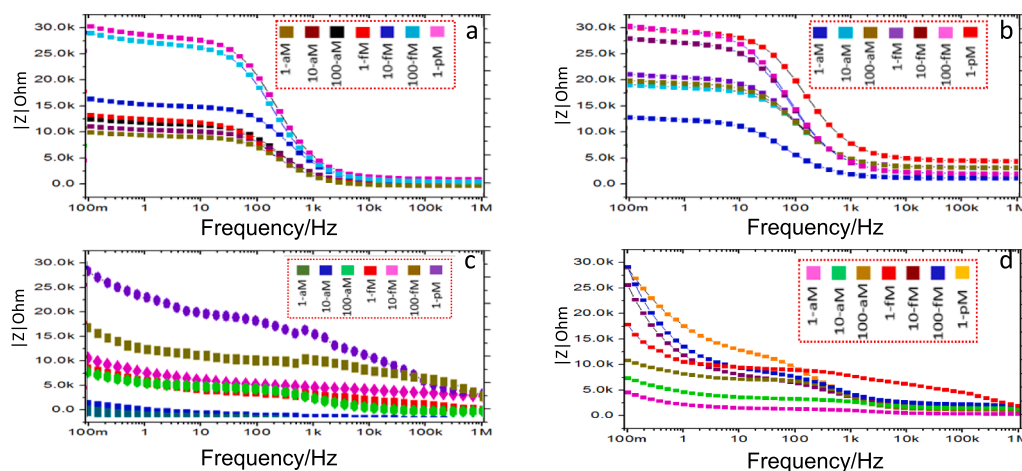
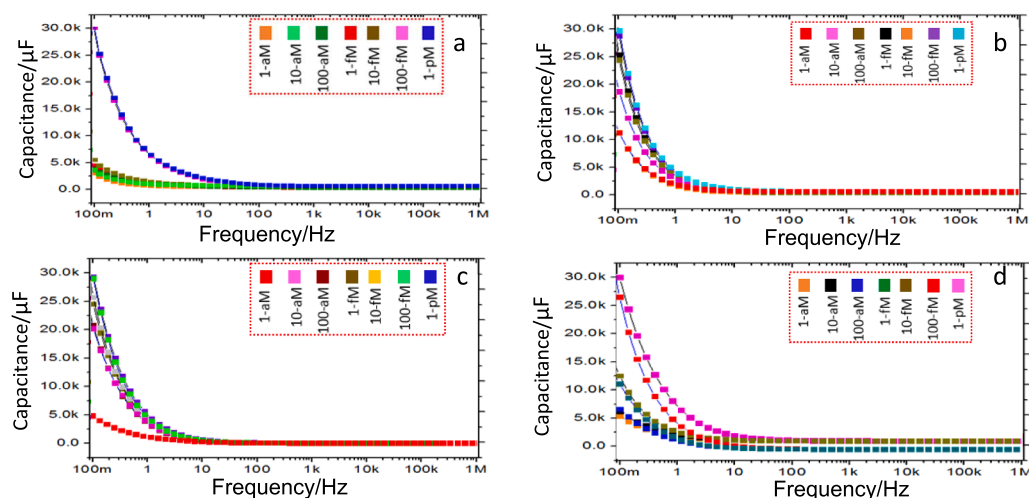


Fig. 5. The study analyzed electrodes from different alpha synuclein concentrations using electrochemical impedance spectroscopy, faradaic and nonfaradaic techniques with frequency vs total impedance: AuIDTEs sensing in faradaic-EIS nonfaradaic mode was evaluated in buffer with Fe(CN) $_6$  and a redox couple. Biasing was achieved. (a) faradic detection of frequency vs total impedance measurement with normal alpha synuclein with linear range from 1-aM to 1-pM, (b) faradic detection of frequency vs total impedance measurement with aggregated alpha synuclein with linear range from 1-aM to 1-pM, (c) non-faradaic plot of frequency vs total impedance for normal alpha synuclein, (d) nonfaradaic plot of frequency vs total impedance for aggregated alpha synuclein.



**Fig. 6.** The sensing performance of faradaic and nonfaradaic EIS detection modes was investigated in a 10 mM PBS buffer (pH 7.4) with electrodes biased at 100 mVrms in the frequency range of 106 Hz down to 0.1 Hz. Nyquist plot for detecting varying levels of alpha synuclein, with an inset figures exhibiting its equivalent circuit. (a) faradaic Bode plot of absolute capacitance versus frequency response for normal alpha synuclein binding at different concentrations, (c) non-faradaic Bode plot of absolute capacitance versus frequency response for aggregated alpha synuclein binding at different concentrations, (d) non-faradaic Bode plot of absolute capacitance versus frequency response for aggregated alpha synuclein binding.

response of the sensor varies at frequencies lower than 10 Hz, demonstrating its activation frequency and insulating features. The capacitance of the electrolyte solution remains constant at frequencies over 101 Hz, however at frequencies below 101 Hz, Cdl values change owing to ion/molecule adsorption. The sensor's capacitance response at 4 Hz is increased by surface pretreatment and increasing alpha synuclein concentration, demonstrating effective target interaction. The study found that the capacitance with the target on the electrode surface changes with frequency, suggesting the presence of the aggregation alpha synuclein. The results showed a clear correlation between the concentration of aggregated alpha synuclein and the absolute capacitance response, indicating the sensitivity and accuracy of faradaic and nonfaradaic techniques in detecting and quantifying amyloid alpha synuclein. This method holds potential for accurate and sensitive detection of alpha synuclein biomarkers, particularly in the early stages of neurodegenerative diseases like Parkinson's disease. The use of AuIDTE in non-faradaic biosensing offers a sensitive and accurate method for

detecting alpha synuclein biomarkers, particularly in the early stages of neurodegenerative diseases such as Parkinson's disease.

### 3.5. Higher performance analysis

Identification of alpha synuclein-associated amyloid fibrils is crucial for diagnosing and monitoring neurological disorders like Parkinson's disease. Accurate and sensitive detection technologies are essential for proper diagnosis and management. Electrochemical approaches, such as faradaic and non-faradaic modes, are commonly used for alpha-synuclein detection, with faradaic mode offering lower detection and quantification limits. The imaginary component ( $\text{Im}(Z)$ ) and real component ( $\text{Re}(Z)$ ) of impedance ( $Z$ ) can provide insights into the sensitivity and reliability of electrochemical techniques for determining LOD and LOQ. The ratio of  $\text{Im}(Z)/[\text{k}\Omega]$  to  $\text{Re}(Z)/[\text{k}\Omega]$  can assess the suitability of a method for detecting and quantifying low concentrations of an analyte. Understanding this ratio across concentration ranges helps

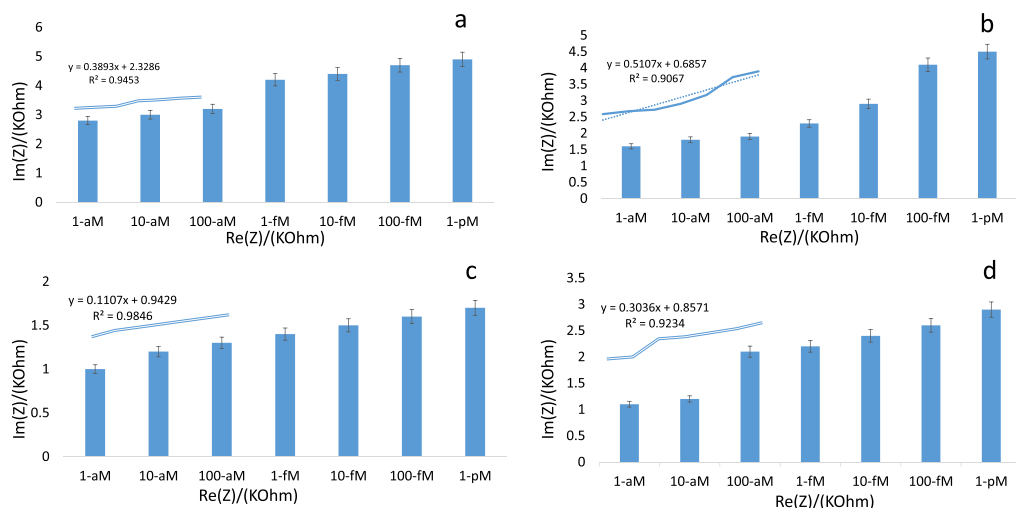


**Fig. 7.** Higher performance analysis: (a) faradaic linear calibration curve for detection of different alpha synuclein concentrations with error bars indicating standard deviations for measured impedance values, (b) faradaic linear calibration curve for detection of different alpha synuclein concentrations with error bars indicating standard deviations for measured impedance values, (c) non-faradaic linear calibration curve for detection of different alpha synuclein concentrations with error bars indicating standard deviations for measured capacitance values, (d) non-faradaic linear calibration curve for detecting various alpha synuclein concentrations, with error bars indicating standard deviations for observed capacitance values.

researchers evaluate analytical methods' performance and ensure reliable detection and quantification of analytes. LOD and LOQ are shown in Fig. 7: LOD for normal alpha synuclein detection in faradaic mode is 2.39-fM with linear relationship of  $R^2 = 0.9453$  (Fig. 7a), LOD for detection of aggregated alpha synuclein in faradaic mode detection is 1.82-fM with linear relationship of  $R^2 = 0.9067$  (Fig. 7b). LOD for non-faradaic detection of normal alpha synuclein is 2.22-fM with linear relationship of  $R^2 = 0.9846$  (Fig. 7c), LOD of non-faradaic detection of aggregated alpha synuclein is 2.40-fM with linear relationship of  $R^2 = 0.9234$  (Fig. 7d), respectively. LOQ for normal alpha synuclein detection in faradaic mode is 7.24-fM, LOQ for aggregated alpha synuclein detection in faradaic mode is 5.52-fM, LOQ of non-faradaic detection of aggregated alpha synuclein is 6.74-fM, and LOQ of non-faradaic detection of aggregated alpha synuclein is 7.27-fM, respectively. Non-faradaic mode, an electrochemical method without redox reactions, has larger detection limitations but can still be helpful in certain situations.  $R^2$  values of 0.9067 and 0.9234 indicate acceptable degree of correlation between the measured data and the fitted model, suggesting a good fit. The study highlights the sensitivity of both faradaic and non-faradaic techniques in detecting amyloid fibrils alpha synuclein. The linear relationships found for both faradaic mode detections highlight the precision and dependability of these electrochemical approaches for detecting alpha-synuclein. Furthermore, the  $R^2$  values observed for normal and aggregated alpha-synuclein detection in faradaic and non-faradaic modes confirm the robustness of these detection approaches. The linear connection in faradaic mode detection of normal alpha synuclein has an  $R^2$  value of 0.9453, indicating a good correlation between the strength of the electrochemical signal and the concentration of normal alpha synuclein. The linear relationship between the electrochemical signal and the concentration of aggregated alpha synuclein in faradaic mode detection has an  $R^2$  value of 0.9067. This suggests that both faradaic and non-faradaic modes can detect and quantify normal and aggregated alpha-synuclein. The results contribute to the existing literature by demonstrating the sensitivity and potential diagnostic uses of electrochemical methods for alpha-synuclein detection. The study also demonstrates the variations in sensitivity and detection limitations between faradaic and non-faradaic electrochemical detection modalities. The findings are consistent with prior research that has demonstrated the use of electrochemical approaches for the detection and monitoring of alpha synuclein in neurological diseases. Electrochemical techniques, alpha-synuclein-based PET imaging, and electroencephalography are potential tools for detecting and monitoring alpha synuclein.

### 3.6. Reproducibility and selectivity

The reproducibility of the immunosensor was investigated by EIS measurements of five individual items and alpha synuclein (1-pM) attached immunosensors. After repeated testing the sensor when the sensor was bare, with CDI, with antibody and with ethanolamine, and with target, the sensor also shown remarkable reproducibility (Fig. 8a). This designates that the immunosensor is promising for the detection of alpha synuclein with high accuracy. Four interfering analysis (bare, CDI, antibody, ethanolamine, and target) and alpha synuclein monomer were examined to investigate the specificity of the sensor. The most essential information in this article is that the developed electrochemical approach demonstrated exceptional selectivity towards alpha synuclein amyloid fibrils. Fig. 8b showed that there were no noticeable differences in  $R_{et}$  values between bare, CDI, antibody, and ethanolamine, on the contrary, the target concentration produced larger signal levels. The Aut showed a remarkable preference for alpha synuclein amyloid fibrils over other macromolecules, showing that the sensor provided was very selective. The selectivity of a sensor was determined by testing two closely related proteins, alpha synuclein and tau. The sensor was found to be selective as no significant change was observed for the control, but the target alpha synuclein showed a significant change. The addition of alpha synuclein amyloid fibrils resulted in a considerable change, revealing the specificity of the sensing method.

### 3.7. Detection of alpha synuclein aggregation in human serum

To show the sensor system's performance in real-world sample analysis, human serum was used as a proof of concept. Actual human serum concentrations in the samples were 1.1109 and  $1.3 \times 10^{-6}$ . The concentrations were  $0.99 \times 10^{-6}$  and  $0.96 \times 10^{-5}$ , respectively. The relative standard deviation (%) ( $n = 3$ ) was 1.18 and 3.89, respectively, with 97.6 and 99.8 as the recovery rate. These results suggest that the sensor is suitable for the application with real samples. There were good recoveries and relative standard deviation (RSD) values. Although this approach may be applied to real materials, numerous types of alpha synuclein protein, including monomers and fibrils, were not investigated in this work. In serum, only alpha synuclein amyloid fibrils was studied.

## 4. Conclusion

The study explores nano-based biosensors for Parkinson's disease using faradaic and non-faradaic techniques. The AuIDTES-based electrochemical assay is a cost-effective, disposable in vitro biosensor with a simple detection principle and low detection limit. The detection of

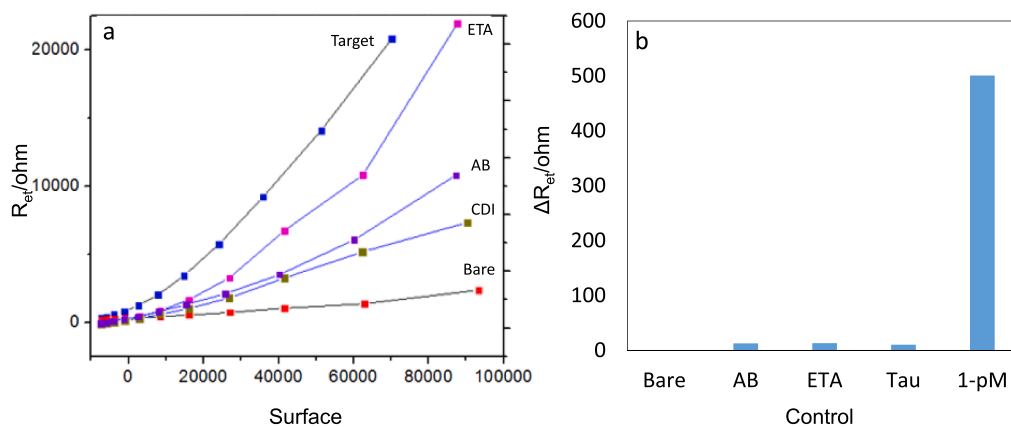


**Fig. 8.** Determination of specificity and reproducibility: (a) reproducibility of the repeated testing of the AuIDTES electrodes surface, (b) the specificity of two closely related proteins, alpha synuclein and tau is compared. The anti-alpha-synuclein antibody identifies only alpha-synuclein; the control protein shows no significant change.



alpha synuclein amyloid fibrils is crucial in the field of neurodegenerative disorders, particularly Parkinson's disease. The selective detection of these fibrils using electrochemical impedance spectroscopic approaches holds great promise for early diagnosis and monitoring of Parkinson's disease progression. This study could achieve enhanced sensitivity, selectivity, and accuracy by using both faradaic and non-faradaic approaches. This can contribute to the development of reliable diagnostic tools and therapeutic strategies for Parkinson's disease, improving patient outcomes and quality of life. The selective detection of alpha synuclein amyloid fibrils can also help understand the underlying mechanisms of other neurodegenerative disorders, such as dementia with Lewy bodies and multiple system atrophy. The development of electrochemical impedance spectroscopic approaches for the selective detection of alpha synuclein amyloid fibrils represents a significant advancement in the field of neurodegenerative disorders, particularly Parkinson's disease.

### CRedit authorship contribution statement

**Hussaini Adam:** Writing – review & editing, Writing – original draft, Validation, Investigation, Formal analysis, Data curation. **Subash C.B. Gopinath:** Writing – review & editing, Visualization, Validation, Supervision, Resources, Project administration, Methodology, Funding acquisition, Conceptualization. **Hemavathi Krishnan:** Writing – review & editing, Validation, Methodology, Formal analysis. **Tijjani Adam:** Writing – review & editing, Visualization, Validation, Resources, Funding acquisition. **Makram A. Fakhri:** Writing – review & editing, Visualization, Validation. **Evan T. Salim:** Writing – review & editing, Visualization, Validation. **A. Shamsher:** Writing – review & editing, Validation, Software, Resources. **Sreeramnan Subramaniam:** Writing – review & editing, Validation. **Yeng Chen:** Writing – review & editing, Validation, Software, Resources.

### Declaration of competing interest

The authors declare that they have no known competing financial interests or personal relationships that could have appeared to influence the work reported in this paper.

### Data availability

No data was used for the research described in the article.

### References

- [1] J. Vaneyck, I. Segers-nolten, K. Broersen, M.M.A.E. Claessens, Cross-seeding of alpha-synuclein aggregation by amyloid fibrils of food proteins, *J. Biol. Chem.* 296 (2021) 100358, <https://doi.org/10.1016/j.jbc.2021.100358>.
- [2] I. Alam, B. Lertanantawong, W. Prongmanee, T. Lertvanithphol, M. Horprathum, T. Sutthibutpong, P. Asanithi, Investigating lysozyme amyloid fibrillization by electrochemical impedance spectroscopy for application in lysozyme sensor, *J. Electroanal. Chem.* 901 (2021) 115799, <https://doi.org/10.1016/j.jelechem.2021.115799>.
- [3] G. Forloni, Alpha synuclein: neurodegeneration and inflammation, *Int. J. Mol. Sci.* 24 (2023), <https://doi.org/10.3390/ijms24065914>.
- [4] M.W. El-Saadi, X. Tian, M. Grames, M. Ren, K. Keys, H. Li, E. Knott, H. Yin, S. Huang, X.H. Lu, Tracing brain genotoxic stress in Parkinson's disease with a novel single-cell genetic sensor, *Sci. Adv.* 8 (2022) 1–21, <https://doi.org/10.1126/sciadv.abd1700>.
- [5] P. Calabresi, G. Di Lazzaro, G. Marino, F. Campanelli, V. Ghiglieri, Advances in understanding the function of alpha-synuclein: implications for Parkinson's disease, *Brain* 146 (2023) 3587–3597, <https://doi.org/10.1093/brain/awad150>.
- [6] Z.D. Zhou, L.X. Yi, D.Q. Wang, T.M. Lim, E.K. Tan, Role of dopamine in the pathophysiology of Parkinson's disease, *Transl. Neurodegener.* 12 (2023) 44, <https://doi.org/10.1186/s40035-023-00378-6>.
- [7] T. Du, L. Wang, W. Liu, G. Zhu, Y. Chen, J. Zhang, Biomarkers and the role of alpha-synuclein in Parkinson's disease, *Front. Aging Neurosci.* 13 (2021) 1–15, <https://doi.org/10.3389/fnagi.2021.645996>.
- [8] T. Hatano, A. Okuzumi, G. Matsumoto, T. Tsunemi, N. Hattori, alpha-Synuclein: a promising biomarker for Parkinson's disease and related disorders, *J. Mov. Disord.* 17 (2024) 127–137, <https://doi.org/10.14802/jmd.24075>.
- [9] A.T. Balana, A.L. Mahul-Mellier, B.A. Nguyen, M. Horvath, A. Javed, E.R. Hard, Y. Jasiqi, P. Singh, S. Afrin, R. Pedretti, V. Singh, V.M.Y. Lee, K.C. Luk, L. Saelices, H.A. Lashuel, M.R. Pratt, O-GlcNAc forces an alpha-synuclein amyloid strain with notably diminished seeding and pathology, *Nat. Chem. Biol.* 20 (2024) 646–655, <https://doi.org/10.1038/s41589-024-01551-2>.
- [10] U. Ganguly, S. Singh, S. Pal, S. Prasad, B.K. Agrawal, R.V. Saini, S. Chakrabarti, Alpha-synuclein as a biomarker of Parkinson's disease: good, but not good enough, *Front. Aging Neurosci.* 13 (2021) 1–19, <https://doi.org/10.3389/fnagi.2021.702639>.
- [11] M. Gómez-Benito, N. Granado, P. García-Sanz, A. Michel, M. Dumoulin, R. Moratalla, Modeling Parkinson's disease with the alpha-synuclein protein, *Front. Pharmacol.* 11 (2020) 1–15, <https://doi.org/10.3389/fphar.2020.00356>.
- [12] D. Sepúlveda, M. Cisternas-Olmedo, J. Arcos, M. Nassif, R.L. Vidal, Contribution of autophagy-lysosomal pathway in the exosomal secretion of alpha-synuclein and its impact in the progression of Parkinson's disease, *Front. Mol. Neurosci.* 15 (2022) 1–15, <https://doi.org/10.3389/fnmol.2022.805087>.
- [13] R. Casella, A. Bigi, N. Cremades, C. Cecchi, Effects of oligomer toxicity, fibril toxicity and fibril spreading in synucleinopathies, *Cell. Mol. Life Sci.* 79 (2022) 1–20, <https://doi.org/10.1007/s00018-022-04166-9>.
- [14] P.R. Christenson, H. Jeong, H. Ahn, M. Li, G. Rowden, R.L. Shoemaker, P.A. Larsen, H.Y. Park, S.-H. Oh, Visual detection of misfolded alpha-synuclein and prions via capillary-based quaking-induced conversion assay (Cap-QuIC), *npj Biosens.* 1 (2024) 2, <https://doi.org/10.1038/s44328-024-00003-0>.
- [15] M. Mcglennen, M. Dieser, C.M. Foreman, S. Warnat, Using electrochemical impedance spectroscopy to study biofilm growth in a 3D-printed flow cell system, *Biosens. Bioelectron.* X 14 (2023) 100326, <https://doi.org/10.1016/j.biosx.2023.100326>.
- [16] A. Kirchhain, A. Bonini, F. Vivaldi, N. Poma, F. Di Francesco, Latest developments in non-faradic impedimetric biosensors: towards clinical applications, *TRAC Trends Anal. Chem.* 133 (2020) 116073, <https://doi.org/10.1016/j.trac.2020.116073>.
- [17] V. Sharma, M.D. Gyanprakash, P. Gupta, J. Ramkumar, Analysis of circuit current in electrochemical micromachining process under the application of different waveforms of pulsed voltage, *J. Manuf. Process.* 75 (2022) 110–124, <https://doi.org/10.1016/j.jmapro.2022.01.006>.
- [18] H.S. Magar, R.Y.A. Hassan, A. Mulchandani, Electrochemical impedance spectroscopy (EIS): Principles, construction, and biosensing applications, *Sensors* 21 (2021), <https://doi.org/10.3390/s21196578>.
- [19] B. Padha, S. Verma, P. Mahajan, S. Arya, Electrochemical impedance spectroscopy (EIS) performance analysis and challenges in fuel cell applications, *J. Electrochem. Sci. Technol.* 13 (2022), <https://doi.org/10.33961/jecst.2021.01263>.
- [20] B.Y. Kaplan, A.C. Kırloğlu, M. Alinezhadfar, M.A. Zabara, N.R. Mojarrad, B. Iskandarani, A. Yürüm, C.S. Ozkan, M. Ozkan, S.A. Gürsel, Hydrogen production via electrolysis: Operando monitoring and analyses, *Chem. Catal.* 3 (2023) 100601, <https://doi.org/10.1016/j.checat.2023.100601>.
- [21] Z. Štukovnik, U. Bren, Recent developments in electrochemical-impedimetric biosensors for virus detection, *Int. J. Mol. Sci.* 23 (2022), <https://doi.org/10.3390/ijms232415922>.
- [22] X. Wang, J. Zhou, H. Wang, Bioreceptors as the key components for electrochemical biosensing in medicine, *Cell Rep. Phys. Sci.* 5 (2024) 101801, <https://doi.org/10.1016/j.xcrp.2024.101801>.
- [23] F. Gao, C. Liu, L. Zhang, T. Liu, Z. Wang, Z. Song, H. Cai, Z. Fang, J. Chen, J. Wang, M. Han, J. Wang, K. Lin, R. Wang, M. Li, Q. Mei, X. Ma, S. Liang, G. Gou, N. Xue, Wearable and flexible electrochemical sensors for sweat analysis: a review, *Microsyst. Nanoeng.* 9 (2023) 1, <https://doi.org/10.1038/s41378-022-00443-6>.
- [24] R. Patel, M. Vinchurkar, A. Mohin Shaikh, R. Patkar, A. Adami, F. Giacomozzi, R. Ramesh, B. Pramanick, L. Lorenzelli, M. Shojaei Baghini, I. Part, Non-faradaic electrochemical impedance-based DNA biosensor for detecting phytopathogen – *Ralstonia solanacearum*, *Bioelectrochemistry* 150 (2023) 108370, <https://doi.org/10.1016/j.bioelechem.2023.108370>.
- [25] Z. Gan, M.A.M. Roslan, M.Y. Abd Shukur, M. Halim, N.A. Yasid, J. Abdullah, I. S. Md Yasin, H. Wasoh, Advances in aptamer-based biosensors and cell-internalizing SELEX technology for diagnostic and therapeutic application, *Biosensors* 12 (2022) 1–17, <https://doi.org/10.3390/bios12110922>.
- [26] N.A. Makoah, T. Tipih, M.M. Litabe, M. Brink, J.B. Sempa, D. Goedhals, F.J. Burt, A systematic review and meta-analysis of the sensitivity of antibody tests for the laboratory confirmation of COVID-19, *Future Virol.* 17 (2022) 119–139, <https://doi.org/10.2217/fvl-2021-0211>.
- [27] D. Calabria, M.M. Calabretta, M. Zangheri, E. Marchegiani, I. Trozzi, M. Guardigli, E. Michelini, F. Di Nardo, L. Anfossi, C. Baggiani, M. Mirasoli, Recent advancements in enzyme-based lateral flow immunoassays, *Sensors* 21 (2021) 1–19, <https://doi.org/10.3390/s21103358>.
- [28] B. Wiltschi, T. Cernava, A. Dennig, M. Galindo Casas, M. Geier, S. Gruber, M. Haberbauer, P. Heidinger, E. Herrero Acero, R. Kratzer, C. Luley-Goedl, C. A. Müller, J. Pitzer, D. Ribitsch, M. Sauer, K. Schmolzer, W. Schnitzhofer, C. W. Sensen, J. Soh, K. Steiner, C.K. Winkler, M. Winkler, T. Wriessnegger, Enzymes revolutionize the bioproduction of value-added compounds: From enzyme discovery to special applications, *Biotechnol. Adv.* 40 (2020) 107520, <https://doi.org/10.1016/j.biotechadv.2020.107520>.
- [29] R.S. Massey, R.R. Appadurai, R. Prakash, A surface imprinted polymer EIS sensor for detecting alpha-synuclein, a Parkinson's disease biomarker, *Micromachines* 15 (2024), <https://doi.org/10.3390/mi15020273>.
- [30] A. Koklu, S. Wustoni, V.E. Musteata, D. Ohayon, M. Moser, I. McCulloch, S. P. Nunes, S. Inal, Microfluidic integrated organic electrochemical transistor with a nanoporous membrane for amyloid-β detection, *ACS Nano* 15 (2021) 8130–8141, <https://doi.org/10.1021/acsnano.0c09893>.

- [31] S.J. Jang, C.S. Lee, T.H. Kim,  $\alpha$ -Synuclein oligomer detection with aptamer switch on reduced graphene oxide electrode, *Nanomaterials* 10 (2020) 1–11, <https://doi.org/10.3390/nano10050832>.
- [32] J.A. Ribeiro, P.A.S. Jorge, Applications of electrochemical impedance spectroscopy in disease diagnosis—A review, *Sens. Actuators Rep.* 8 (2024) 100205, <https://doi.org/10.1016/j.snr.2024.100205>.
- [33] M.A. Ehsan, S.A. Khan, A. Rehman, Screen-printed graphene/carbon electrodes on paper substrates as impedance sensors for detection of coronavirus in nasopharyngeal fluid samples, *Diagnostics* 11 (2021), <https://doi.org/10.3390/diagnostics11061030>.
- [34] J.S. Park, H.J. Kim, J.H. Lee, J.H. Park, J. Kim, K.S. Hwang, B.C. Lee, Amyloid beta detection by faradaic electrochemical impedance spectroscopy using interdigitated microelectrodes, *Sensors (Switzerland)* 18 (2018), <https://doi.org/10.3390/s18020426>.
- [35] L.O. Orzari, L.R.G.E. Silva, R.C. de Freitas, L.C. Brazaca, B.C. Janegitz, Lab-made disposable screen-printed electrochemical sensors and immunosensors modified with Pd nanoparticles for Parkinson's disease diagnostics, *Mikrochim. Acta* 191 (2024) 76, <https://doi.org/10.1007/s00604-023-06158-3>.
- [36] M. Dhinesh, M. Karthikeyan, N. Sharma, V. Raju, J. Vatsalarani, S.V. Kalivendi, C. Karunakaran, Molecular imprinting synthetic receptor based sensor for determination of Parkinson's disease biomarker DJ-1, *Microchem. J.* 183 (2022) 107959, <https://doi.org/10.1016/j.microc.2022.107959>.
- [37] M. Dhinesh Kumar, M. Karthikeyan, G. Kaniraja, P. Ananthappan, V.S. Vasantha, C. Karunakaran, Screening and comparative studies of conducting polymers for developing effective molecular imprinted sensors for copper, zinc superoxide dismutase, *Sens. Actuators, B Chem.* 391 (2023) 134007, <https://doi.org/10.1016/j.snb.2023.134007>.
- [38] G.C.M. de Oliveira, J.H.S. de Carvalho, L.C. Brazaca, N.C.S. Vieira, B.C. Janegitz, Flexible platinum electrodes as electrochemical sensor and immunosensor for Parkinson's disease biomarkers, *Biosens. Bioelectron.* 152 (2020) 112016, <https://doi.org/10.1016/j.bios.2020.112016>.
- [39] M. Wen, Y. Xing, G. Liu, S. Hou, S. Hou, Electrochemical sensor based on Ti3C2 membrane doped with UiO-66-NH2 for dopamine, *Microchim. Acta* 189 (2022) 1–8, <https://doi.org/10.1007/s00604-022-05222-8>.